# Crystal-field analysis of the magnetization process in a series of $Nd_2Fe_{14}B$-type compounds

Motohiko Yamada, Hiroaki Kato, Hisao Yamamoto, and Yasuaki Nakagawa
*Institute for Materials Research, Tohoku University, Sendai 980, Japan*
(Received 4 November 1987)

A systematic study of the magnetic properties of a series of $R_2Fe_{14}B$ ($R$ denotes a rare-earth element) compounds has been made using a combined molecular-field and crystalline-electric-field (CEF) approximation. The Hamiltonian for an $R$ ion is (in units of $\mu_B$) $\mathcal{H}_R=\lambda\mathbf{L}\cdot\mathbf{S}+\mathcal{H}_{\rm CEF}+2\mathbf{S}\cdot\mathbf{H}_m+(\mathbf{L}+2\mathbf{S})\cdot\mathbf{H}$, where $\mathcal{H}_{\rm CEF}$ is the CEF Hamiltonian and $\mathbf{H}_m$ is the molecular field acting on the $R$ ion due to the Fe-$R$ exchange interaction. We have calculated the spin structure and magnetization curves using the Racah method, taking the excited $J$ multiplets into account. The experimental results are explained satisfactorily in terms of almost the same CEF parameters. For the heavy-$R$ compounds the Stevens method can be applied. The sixth-order CEF parameters are indispensable to explain the anomalous magnetization increase observed in the Sm compound and the first-order magnetization process (FOMP) observed in the Nd and Pr compounds. The excited $J$ multiplets are shown to have an appreciable influence on the FOMP.

## I. INTRODUCTION

Recently magnetic properties of $R_2Fe_{14}B$ ($R$ denotes a rare-earth element) compounds have been studied extensively in connection with the Nd-Fe-B permanent magnet.[1] The $R_2Fe_{14}B$ compounds have a tetragonal structure with space group $P4_2/mnm$.[2,3] Since the ferromagnetic Curie temperatures of $R_2Fe_{14}B$ are nearly the same as that of $Y_2Fe_{14}B$ (Refs. 4–7) which contains only Fe as magnetic ions, the magnetic ordering is presumed to be dominated mostly by the strong Fe-Fe exchange interaction. In general the magnetic moments of $R$ and Fe are parallel in the light-$R$ compounds and antiparallel in the heavy-$R$ compounds because of the antiferromagnetic exchange interaction between the spin magnetic moments of $R$ and Fe. In some cases, however, the moments become noncollinear since the $R$ moments exhibit a large magnetic anisotropy due to the crystalline electric field (CEF). The anisotropy of $Ce_2Fe_{14}B$ (Ref. 8) and $Gd_2Fe_{14}B$ (Ref. 9) is similar to that of the Y compound, because Ce is in the tetravalent state in the compound, losing $4f$ electrons, and Gd has no orbital moment. The Fe-$R$ exchange interaction is weaker than the Fe-Fe interaction[9] but much stronger than the $R$-$R$ interaction. Hence, the $R$-$R$ exchange interaction may be neglected. A wide variety of magnetic properties of this series of compounds arises from the magnetic $R$ ion being subjected simultaneously to CEF and an Fe-$R$ exchange field.

In the compounds with Nd,[4] and Ho,[5] the magnetization vectors at 0 K are tilted from the $c$ axis at about 32° and 23°, respectively. The tilting angles of the two compounds decrease monotonically with increasing temperature, and become zero at 135 K and 58 K, respectively. In the compounds with Er,[5,10] Tm,[5] and Yb,[11] the magnetization vectors lie in the $c$ plane at low temperatures, and the directions change to the $c$ axis at 323, 315, and 115 K, respectively. These temperatures are called the spin-reorientation (SR) temperatures ($T_s$). In the Sm compound,[6,7,12] the magnetization vector lies in the $c$ plane up to (at least) 450 K, while those of the Pr,[8] Tb,[6,13,14] and Dy (Refs. 13 and 14) compounds are parallel to the $c$ axis up to the Curie temperature.

From the magnetization measurements it has become clear that the anisotropy energies of the Sm, Tb, and Dy compounds are so large that a magnetic field of about 150 kOe is insufficient to saturate the magnetization in the hard direction even at room temperature. On the other hand, for the compounds with Pr, Nd, Ho, Er, and Tm a lower field is sufficient to saturate the magnetization in the hard direction at room temperature. The apparent saturation values, however, are different between the easy and hard directions. At low temperatures the anisotropy energies of this series are so large that an extremely high field is necessary to examine the magnetization process. For the compounds with Ho, Er, and Tm the magnetization curve in the hard direction increases monotonically without any indication of saturation up to 145 kOe, and is expected to cross the magnetization curve in the easy direction above 150 kOe at 4.2 K.

Pareti *et al.*[15] observed the first-order magnetization process (FOMP) in the Nd compound with pulsed high magnetic fields applied in the $c$ plane without specifying the direction in the $c$ plane. Kajiwara *et al.*[16,17] reexamined the magnetization process in this compound and found no anomalous magnetization in the [110] direction up to 300 kOe, while in the [100] direction the magnetization jump was observed at about 170 kOe at 77 K. Hiroyoshi *et al.*[18] observed the FOMP in the Pr compound in the [100] and [110] directions at about 130 and 160 kOe, respectively, at 4.2 K.

A Hamiltonian to describe an $R$ ion in a CEF is conventionally written as

$$\mathcal{H}_{\rm CEF}=\sum_{n,m} B_n^m O_n^m \ , \tag{1}$$

within the ground $J$ multiplet, where $O_n^m$ is Stevens operator[19] and $B_n^m$ is CEF coefficient. The directions of

 

magnetization vectors of the Pr, Sm, Tb, Dy, Er, Tm, and Yb compounds at low temperatures and those of the Nd and Ho compounds above $T_s$ are consistent with the sign of the second-order CEF coefficients $B_2^0$ (Refs. 4 and 20) expected from the CEF caused by $R^{3+}$ point charges. It is, therefore, expected that a CEF Hamiltonian which includes the higher terms beyond $B_2^0$ can explain the wide variation in magnetic properties of this series. Some work has been done in this framework.[4,18,21–25]

In Sec. II we present a general formulation of the problem, including excited $J$ multiplets of the $R$ ions. A procedure for the calculation of the spin structure and magnetization is described. In Sec. III the qualitative results are given for a case in which the Fe-$R$ exchange interaction is much stronger than the CEF potential of an $R$ ion. In Sec. IV the results of calculation for the spin structure and magnetization process are quantitatively shown and compared with experimental results. A discussion about the influence of the excited $J$ multiplets on the magnetization process is given in Sec. V, especially on the FOMP observed in the Nd and Pr compounds.

## II. FORMULATION

The crystal structure of $R_2Fe_{14}B$ is shown in Fig. 1, where the Fe ion sites are omitted for clarity.[2,3] There are two crystallographic sites $f$ and $g$ for $R$ ions, which

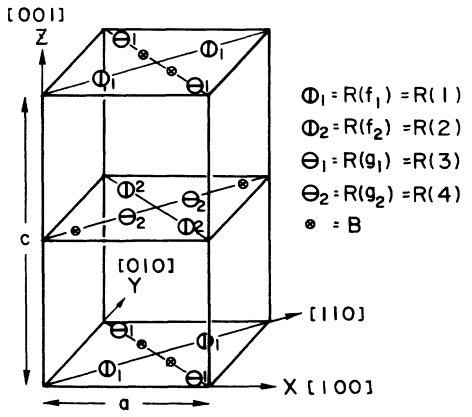


FIG. 1. Chemical unit cell of $R_2Fe_{14}B$. Four $R$-ion sites $f_1$, $f_2$, $g_1$, and $g_2$ are designated by symbols $\Phi_1$, $\Phi_2$, $\Theta_1$, and $\Theta_2$, respectively, and B ions by $\otimes$. Fe ions are omitted.

are further subdivided magnetically into $f_1$, $f_2$, $g_1$, and $g_2$ sites. Therefore, it is necessary to deal with a spin system composed of four $R$ ions and 28 Fe ions, i.e., $2R_2Fe_{14}B$. Since the CEF of the $R$ ion has an orthorhombic symmetry, the Hamiltonian describing the CEF potential of the $R(i)$ ion at the $i$th site ($i=1-4$ denoting $f_1, f_2, g_1, g_2$) is expressed by

$$\begin{aligned}\mathcal{H}_{\mathrm{CEF}}(i)=&A_2^0(i)\sum_j(3z_j^2-r_j^2)+A_2^{-2}(i)\sum_j 2x_jy_j+A_4^0(i)\sum_j(35z_j^4-30r_j^2z_j^2+3r_j^4)\\&+A_4^{-2}(i)\sum_j(7z_j^2-r_j^2)2x_jy_j+A_4^4(i)\sum_j(x_j^4-6x_j^2y_j^2+y_j^4)+A_6^0(i)\sum_j(231z_j^6-315r_j^2z_j^4+105r_j^4z_j^2-5r_j^6)\\&+A_6^{-2}(i)\sum_j(33z_j^4-18r_j^2z_j^2+r_j^4)2x_jy_j+A_6^4(i)\sum_j(11z_j^2-r_j^2)(x_j^4-6x_j^2y_j^2+y_j^4)\\&+A_6^{-6}(i)\sum_j(6x_j^5y_j-20x_j^3y_j^3+6x_jy_j^5)\ ,\end{aligned}\tag{2}$$

where the summation $j$ is over all the $4f$ electrons. The $A_n^m$ are the coefficients of the spherical harmonics of the CEF. Owing to the symmetry of the crystal structure, the following relations hold between the $R(1)$ and $R(2)$ ions

$$A_n^{-2}(1)=-A_n^{-2}(2)\quad(n=2,4,6),\quad A_6^{-6}(1)=-A_6^{-6}(2)\ ,\tag{3}$$

and similar relations between the $R(3)$ and $R(4)$ ions are also obtained.

### A. Hamiltonian for the lowest $J$ multiplet

Within the lowest $J$ multiplet the CEF Hamiltonian is simply given by Eq. (1), i.e.,

$$\begin{aligned}\mathcal{H}_{\mathrm{CEF}}(i)=&B_2^0(i)O_2^0+B_2^{-2}(i)O_2^{-2}+B_4^0(i)O_4^0+B_4^{-2}(i)O_4^{-2}\\&+B_4^4(i)O_4^4+B_6^0(i)O_6^0+B_6^{-2}(i)O_6^{-2}\\&+B_6^4(i)O_6^4+B_6^{-6}(i)O_6^{-6}\ ,\end{aligned}\tag{4}$$

and

$$B_n^m=\theta_n\langle r^n\rangle A_n^m\ ,\tag{5}$$

where $\theta_n$ is the Stevens factors $\alpha,\beta,\gamma$ for $n=2,4,6$, respectively, and $\langle r^n\rangle$ the average of $r^n$ over the radial wave function of the $4f$ electrons.[26,27] Then the Hamiltonian to describe the whole system is given by[13,18,22] (in units of $\mu_B$)

$$\mathcal{H}=\sum_{i=1}^{4}\mathcal{H}_R(i)+28K_0(T)\sin^2\theta-28\mathbf{m}_0(T)\cdot\mathbf{H}\ ,\tag{6}$$

$$\mathcal{H}_R(i)=\mathcal{H}_{\mathrm{CEF}}(i)+2(g_J-1)\mathbf{J}\cdot\mathbf{H}_m+g_J\mathbf{J}\cdot\mathbf{H}\ ,\tag{7}$$

where $\mathbf{m}_0(T)$ is the magnetic moment of an Fe ion at temperature $T$, $\mathbf{H}$ the external magnetic field, $K_0(T)$ the uniaxial anisotropy energy per Fe ion, $\theta$ the angle between $\mathbf{m}_0$ and the [001] direction, and $\mathbf{H}_m$ the molecular field (antiparallel to $\mathbf{m}_0$) due to the Fe-$R$ exchange interaction acting on the reference $R$ ion with $J$ and $g_J$. The Y compound, which contains only Fe ions as magnetic ions, suggests that the Fe sublattice in $R_2Fe_{14}B$ is dominated

mostly by the strong Fe-Fe interaction, so that it is reasonable to assume that the Fe-$R$ exchange interaction does not affect the Fe sublattice very much. Therefore, the temperature dependence of $K_0$ and $\mathbf{m}_0$ in the $R$ compounds is assumed to be identical with that in $Y_2Fe_{14}B$,[5] although the temperature scale must, of course, be renormalized depending on the magnitude of the Curie temperature.

Since the interplay of $\mathbf{H}_m$ and $B_n^m$ is important in $R_2Fe_{14}B$, the eigenvalues of the $\mathcal{H}_R(i)$ are obtained by diagonalizing the $(2J+1)\times(2J+1)$ matrix in the $|J,M\rangle$ representation. The calculation of the matrix elements $\langle J,M|\mathcal{H}_R(i)|J,M'\rangle$ is straightforward because the operator $O_n^m$ is expressed in terms of $J_\pm=J_x\pm iJ_y$ and $J_z$. For example, $O_2^0=3J_z^2-J(J+1)$, $O_2^{-2}=(J_+^2-J_-^2)/2i$, etc.[28]

The equilibrium state of the system is determined by the following procedure. The directions $(\Theta,\Phi)$ of an external magnetic field and $(\theta,\phi)$ of the magnetic moment of the Fe ion are taken as shown in Fig. 2. The eigenvalues and eigenfunctions of $\mathcal{H}_R(i)$ for a given $(\theta,\phi)$ are obtained by diagonalizing the $(2J+1)\times(2J+1)$ matrix of $\mathcal{H}_R(i)$.

$$\mathcal{H}_R(i)|i,s\rangle=E_s(i)|i,s\rangle,\quad s=1,2,\ldots,2J+1$$
$$|i,s\rangle=\sum_M a_{JM}^s|J,M\rangle,\quad \sum_M|a_{JM}^s|^2=1\ . \tag{8}$$

The free energy of the system is given by

$$F(\mathbf{H},\mathbf{H}_m,T)=-kT\sum_{i=1}^{4}\ln Z(i)+28K_0(T)\sin^2\theta - 28\mathbf{m}_0(T)\cdot\mathbf{H}\ ,$$
$$Z(i)=\sum_{s=1}^{2J+1}\exp[-E_s(i)/kT]\ . \tag{9}$$

Then we find the equilibrium direction of the molecular field $(\theta_0,\phi_0)$, which makes the free-energy minimum, i.e.,

$$F(\Theta,\Phi,\theta_0,\phi_0,H,T)=-kT\sum_{i=1}^{4}\ln Z(i)+28K_0(T)\sin^2\theta_0 - 28m_0(T)H[\sin\Theta\sin\theta_0\cos(\Phi-\phi_0)+\cos\Theta\cos\theta_0]\ . \tag{10}$$

The magnetic moments of $R(i)$ ions are thus given by

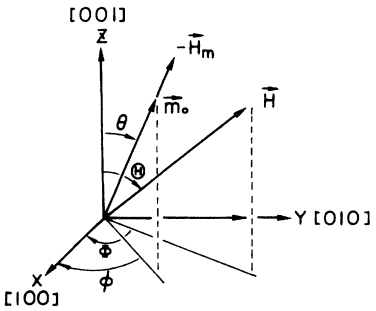


FIG. 2. Schematic representation of an external field $\mathbf{H}=(H,\Theta,\Phi)$, magnetic moment of an Fe ion $\mathbf{m}_0=(m_0,\theta,\phi)$ and molecular field $\mathbf{H}_m$ which is antiparallel to $\mathbf{m}_0$, i.e., $-\mathbf{H}_m=(H_m,\theta,\phi)$.

$$m_{i\gamma}=-\sum_s(i,s|J_\gamma|i,s)g_J\exp[-E_s(i)/kT]/Z(i)\qquad(\gamma=x,y,z)$$
$$=-\sum_s\sum_{M,M'}a_{JM'}^{s*}(i)a_{JM}^s(i)\langle J,M'|J_\gamma|J,M\rangle g_J\times\exp[-E_s(i)/kT]/Z(i)\ . \tag{11}$$

The spin structure of $R_2Fe_{14}B$ at any temperature is determined when the calculation is made for $H=0$. The magnetic moment of the system ($2R_2Fe_{14}B$) along the field direction is given by

$$M(\mathbf{H})=28m_0(T)[\sin\Theta\sin\theta_0\cos(\Phi-\phi_0)+\cos\Theta\cos\theta_0]+\sum_{i=1}^{4}[m_{ix}\sin\Theta\cos\Phi+m_{iy}\sin\Theta\sin\Phi+m_{iz}\cos\Theta]\ . \tag{12}$$

### B. Hamiltonian including excited $J$ multiplets

Next, we consider a more general treatment for the system in which excited $J$ multiplets are also taken into account.[29–31] The general Hamiltonian for an $R(i)$ ion is given by

$$\mathcal{H}_R(i)=\lambda\mathbf{L}\cdot\mathbf{S}+\mathcal{H}_{\rm CEF}(i)+2\mathbf{S}\cdot\mathbf{H}_m+(\mathbf{L}+2\mathbf{S})\cdot\mathbf{H}\ , \tag{13}$$

instead of Eq. (7). Here $\mathcal{H}_{\rm CEF}(i)$ is given by Eq. (2) instead of Eq. (4). The matrix elements of $\mathcal{H}_{\rm CEF}$ can be calculated using the tensor-operator technique developed by Racah.[32,33] In terms of the spherical harmonics

$$Y_n^m(\theta,\phi)=\left[\frac{2n+1}{4\pi}\right]^{1/2}U_n^m(\theta,\phi)\ , \tag{14}$$

Eq. (2) is expressed by

$$\begin{aligned}\mathcal{H}_{\rm CEF}=&A_2^0\sum_j r_j^2 2U_2^0(\theta_j,\phi_j)+iA_2^{-2}\sum_j r_j^2(\tfrac{2}{3})^{1/2}[U_2^{-2}(\theta_j,\phi_j)-U_2^2(\theta_j,\phi_j)]+A_4^0\sum_j r_j^4 8U_4^0(\theta_j,\phi_j)\\&+iA_4^{-2}\sum_j r_j^4 2(\tfrac{2}{5})^{1/2}[U_4^{-2}(\theta_j,\phi_j)-U_4^2(\theta_j,\phi_j)]+A_4^4\sum_j r_j^4 4(\tfrac{2}{35})^{1/2}[U_4^{-4}(\theta_j,\theta_j)+U_4^4(\theta_j,\phi_j)]\\&+A_6^0\sum_j r_j^6 16U_6^0(\theta_j,\phi_j)+iA_6^{-2}\sum_j r_j^6 16(\tfrac{1}{105})^{1/2}[U_6^{-2}(\theta_j,\phi_j)-U_6^2(\theta_j,\phi_j)]\\&+A_6^4\sum_j r_j^6\tfrac{8}{21}14^{1/2}[U_6^{-4}(\theta_j,\phi_j)+U_6^4(\theta_j,\phi_j)]+iA_6^{-6}\sum_j r_j^6 16(\tfrac{1}{231})^{1/2}[U_6^{-6}(\theta_j,\phi_j)-U_6^6(\theta_j,\phi_j)]\ .\end{aligned} \tag{15}$$

The $LSJM$ matrix elements of $\sum r_j^n U_n^m(\theta_j,\phi_j)$ are given by[30,34]

$$\langle 4f^k,L,S,J,M \mid \sum_j r_j^n U_n^m(\theta_j,\phi_j) \mid 4f^k,L,S,J',M' \rangle$$
$$=(-1)^{L+S-M+J-J'}[(2J+1)(2J'+1)]^{1/2}\begin{pmatrix} J & J' & n \\ -M & M' & m \end{pmatrix}\begin{Bmatrix} L & L & n \\ J & J' & S \end{Bmatrix}\langle 4f^k,L,S\|U_n\|4f^k,L,S\rangle\langle r^n\rangle , \quad (16)$$

where the large parentheses and large curly brackets denote the Wigner $3j$ and $6j$ symbols,[34] respectively, and $\langle\|U_n\|\rangle$ is the reduced matrix element[29] given in Table I. Within the ground $LS$ multiplet the reduced matrix element $\langle\|U_n\|\rangle$ does not depend on $J$ and $M$. The final form of the CEF Hamiltonian for the ground $LS$ multiplet is expressed by

$$\mathcal{H}_{\rm CEF}=C_2^0U(2,0)+iC_2^{-2}[U(2,-2)-U(2,2)]+C_4^0U(4,0)+iC_4^{-2}[U(4,-2)-U(4,2)]+C_4^4[U(4,-4)+U(4,4)]$$
$$+C_6^0U(6,0)+iC_6^{-2}[U(6,-2)-U(6,2)]+C_6^4[U(6,-4)+U(6,4)]+iC_6^{-6}[U(6,-6)-U(6,6)] , \quad (17)$$

where the matrix element of $U(n,m)$ is given by

$$\langle L,S,J,M \mid U(n,m) \mid L,S,J',M'\rangle=(-1)^{L+S-M+J-J'}[(2J+1)(2J'+1)]^{1/2}\begin{pmatrix} J & J' & n \\ -M & M' & m \end{pmatrix}\begin{Bmatrix} L & L & n \\ J & J' & S \end{Bmatrix} . \quad (18)$$

The relations between $C_n^m$ and $A_n^m(B_n^m)$ are given by

$$\begin{aligned}
&C_2^0=A_2^0\langle r^2\rangle 2\langle\|U_2\|\rangle=B_2^0 2\langle\|U_2\|\rangle/\alpha ,\\
&C_2^{-2}=A_2^{-2}\langle r^2\rangle(\tfrac{2}{3})^{1/2}\langle\|U_2\|\rangle=B_2^{-2}(\tfrac{2}{3})^{1/2}\langle\|U_2\|\rangle/\alpha ,\\
&C_4^0=A_4^0\langle r^4\rangle 8\langle\|U_4\|\rangle=B_4^0 8\langle\|U_4\|\rangle/\beta ,\\
&C_4^{-2}=A_4^{-2}\langle r^4\rangle 2(\tfrac{2}{5})^{1/2}\langle\|U_4\|\rangle=B_4^{-2}2(\tfrac{2}{5})^{1/2}\langle\|U_4\|\rangle/\beta ,\\
&C_4^4=A_4^4\langle r^4\rangle 4(\tfrac{2}{35})^{1/2}\langle\|U_4\|\rangle=B_4^4 4(\tfrac{2}{35})^{1/2}\langle\|U_4\|\rangle/\beta ,\\
&C_6^0=A_6^0\langle r^6\rangle 16\langle\|U_6\|\rangle=B_6^0 16\langle\|U_6\|\rangle/\gamma ,\\
&C_6^{-2}=A_6^{-2}\langle r^6\rangle 16(\tfrac{1}{105})^{1/2}\langle\|U_6\|\rangle=B_6^{-2}16(\tfrac{1}{105})^{1/2}\langle\|U_6\|\rangle/\gamma ,\\
&C_6^4=A_6^4\langle r^6\rangle\tfrac{8}{21}14^{1/2}\langle\|U_6\|\rangle=B_6^4\tfrac{8}{21}14^{1/2}\langle\|U_6\|\rangle/\gamma ,\\
&C_6^{-6}=A_6^{-6}\langle r^6\rangle 16(\tfrac{1}{231})^{1/2}\langle\|U_6\|\rangle=B_6^{-6}16(\tfrac{1}{231})^{1/2}\langle\|U_6\|\rangle/\gamma ,
\end{aligned} \quad (19)$$

where the second expression for $C_6^m$ expressed in terms of $B_6^m$ is used only when $\gamma\neq 0$.

The Stevens factor $\theta_n$ for a given $J$ multiplet is expressed by

$$\theta_n^J=(-1)^{L+S+J}2^n(2J+1)\left[\frac{(2J-n)!}{(2J+n+1)!}\right]^{1/2}\begin{Bmatrix} L & L & n \\ J & J & S \end{Bmatrix}\langle f^k,S,L\|U_n\|f^k,S,L\rangle, \quad n=2,4,6 \quad (20)$$

TABLE I. Reduced matrix elements of the lowest $SL$ term of the $R^{3+}$ ions. The upper sign corresponds to the upper ion of each pair. Our definitions differ by numerical factors from those of Ref. 29 (table of reduced matrix elements in Ref. 29 contains some errors).

| $R^{3+}$ | $f^k$ | $^{2S+1}L$ | $\langle SL\|U_2\|SL\rangle$ | $\langle SL\|U_4\|SL\rangle$ | $\langle SL\|U_6\|SL\rangle$ |
|---|---|---|---|---|---|
| $Ce^{3+}$<br>$Yb^{3+}$ | $f^1$<br>$f^{13}$ | $^2F$ | $\mp 2(\frac{7}{15})^{1/2}$ | $\pm(\frac{14}{11})^{1/2}$ | $\mp 10[(7)/(3)(11)(13)]^{1/2}$ |
| $Pr^{3+}$<br>$Tm^{3+}$ | $f^2$<br>$f^{12}$ | $^3H$ | $\mp\frac{1}{3}[(2)(11)(13)/(15)]^{1/2}$ | $\mp\frac{2}{3}[(2)(13)/(11)]^{1/2}$ | $\pm\frac{10}{3}[(5)(17)/(3)(11)(13)]^{1/2}$ |
| $Nd^{3+}$<br>$Er^{3+}$ | $f^3$<br>$f^{11}$ | $^4I$ | $\mp[(2)(7)(13)/(3)(11)(15)]^{1/2}$ | $\mp[(4)(7)(13)(17)/(3)^2(11)^3]^{1/2}$ | $\mp\frac{50}{11}[(17)(19)/(3)^2(11)(13)]^{1/2}$ |
| $Pm^{3+}$<br>$Ho^{3+}$ | $f^4$<br>$f^{10}$ | $^5I$ | $\pm[(2)(7)(13)/(3)(11)(15)]^{1/2}$ | $\pm[(4)(7)(13)(17)/(3)^2(11)^3]^{1/2}$ | $\pm\frac{50}{11}[(17)(19)/(13)^2(11)(13)]^{1/2}$ |
| $Sm^{3+}$<br>$Dy^{3+}$ | $f^5$<br>$f^9$ | $^6H$ | $\pm\frac{1}{3}[(2)(11)(13)/(15)]^{1/2}$ | $\pm\frac{2}{3}[(2)(13)/(11)]^{1/2}$ | $\mp\frac{10}{3}[(5)(17)/(3)(11)(13)]^{1/2}$ |
| $Eu^{3+}$<br>$Tb^{3+}$ | $f^6$<br>$f^8$ | $^7F$ | $\pm 2(\frac{7}{15})^{1/2}$ | $\mp(\frac{14}{11})^{1/2}$ | $\pm 10[(7)/(3)(11)(13)]^{1/2}$ |

General expressions for the matrix elements of the Stevens operators $O_n^m$ are simply given by

$$\langle J,M \mid O_2^m \mid J,M' \rangle = (-1)^{J+M}\frac{1}{2}\left[\frac{(2J+3)!}{(2J-2)!}\right]^{1/2}\begin{pmatrix} J & J & 2 \\ -M & M' & m \end{pmatrix}, \tag{21a}$$

$$\langle J,M \mid O_4^m \mid J,M' \rangle = (-1)^{J+M}\frac{1}{2}\left[\frac{(2J+5)!}{(2J-4)!}\right]^{1/2}\begin{pmatrix} J & J & 4 \\ -M & M' & m \end{pmatrix}, \tag{21b}$$

$$\langle J,M \mid O_6^m \mid J,M' \rangle = (-1)^{J+M}\frac{1}{2}\left[\frac{(2J+7)!}{(2J-6)!}\right]^{1/2}\begin{pmatrix} J & J & 6 \\ -M & M' & m \end{pmatrix}. \tag{21c}$$

The matrix elements of the spin-orbit term in the Hamiltonian $\mathcal{H}_R(i)$ are given by

$$\langle L,S,J,M \mid \lambda \mathbf{L}\cdot\mathbf{S} \mid L,S,J',M' \rangle = E_J \delta_{JJ'}\delta_{MM'}, \tag{22}$$

where

$$E_J = \frac{\lambda}{2}[J(J+1)-L(L+1)-S(S+1)] \tag{23}$$

is the energy of the $J$ multiplet state designated by $^{2S+1}L_J$. The nondiagonal $J, J+1$ matrix elements of $S_\gamma$ ($\gamma = x,y,z$) are given by[31]

$$\langle J+1,M \mid S_z \mid J,M \rangle = f(L,S,J,M),$$

$$\langle J+1,M\pm1 \mid S_x \mid J,M \rangle = \mp\tfrac{1}{2} f(L,S,J,M)\left[\frac{(J\pm M+1)(J\pm M+2)}{(J+M+1)(J-M+1)}\right]^{1/2},$$

$$\langle J+1,M\pm1 \mid S_y \mid J,M \rangle = \frac{i}{2} f(L,S,J,M)\left[\frac{(J\pm M+1)(J\pm M+2)}{(J+M+1)(J-M+1)}\right]^{1/2},$$

$$f(L,S,J,M) = \left[\frac{(J+L+S+2)(-J+S+L)(J+S-L+1)(J+L-S+1)(J+M+1)(J-M+1)}{4(J+1)^2(2J+1)(2J+3)}\right]^{1/2}. \tag{24}$$

The following relations hold between the matrix elements of $S_\gamma$ and $L_\gamma$:

$$\langle J+1,M' \mid L_\gamma \mid J,M \rangle = -\langle J+1,M' \mid S_\gamma \mid J,M \rangle. \tag{25}$$

The eigenvalues and eigenfunctions of the $R(i)$ ion are obtained by diagonalizing the $\sum_J (2J+1)\times\sum_J(2J+1)$ matrix of $\mathcal{H}_R(i)$, given by Eq. (13), as

$$\mathcal{H}_R(i) \mid i,s) = E_s(i) \mid i,s), \quad s = 1,2,\ldots,\sum_J (2J+1)$$
$$\mid i,s) = \sum_J \sum_M a_{JM}^s \mid J,M \rangle, \quad \sum_J \sum_M \mid a_{JM}^s \mid^2 = 1. \tag{26}$$

The equilibrium state of the system is determined by the same procedure as used for the case in which only the ground $J$ multiplet was taken into account.

The magnetic moments of $R(i)$ ions are given by

$$m_{i\gamma} = -\sum_s (i,s \mid J_\gamma + S_\gamma \mid i,s)\exp[-E_s(i)/kT]/Z(i)$$
$$= \sum_J m_{i\gamma}(J) - \delta S_{i\gamma}, \quad \gamma = x,y,z \tag{27}$$

instead of Eq. (11), where

$$m_{i\gamma}(J) = -\sum_s \sum_{M,M'} a_{JM'}^{s*}(i) a_{JM}^s(i)\langle J,M' \mid J_\gamma \mid J,M \rangle g_J \times \exp[-E_s(i)/kT]/Z(i), \tag{28}$$

$$-\delta S_{i\gamma} = -\sum_s \sum_{\substack{J,J' \\ (J\neq J')}} \sum_{M,M'} a_{J'M'}^{s*}(i) a_{JM}^s(i)\langle J',M' \mid S_\gamma \mid J,M \rangle \times \exp[-E_s(i)/kT]/Z(i), \tag{29}$$

$$Z(i) = \sum_{s=1}^{\sum_J (2J+1)} \exp[-E_s(i)/kT]. \tag{30}$$

The first term, $\mathbf{m}(J)$, of the second line in Eq. (27) represents the magnetic moment which belongs to each $J$ multiplet. The second term, $-\delta\mathbf{S}$, represents the magnetic moment arising from the intermultiplet interactions.

## III. QUALITATIVE RESULTS: SPIN STRUCTURE AND ANISOTROPY CONSTANT

Since the interplay of $\mathbf{H}_m$ and $A_n^m$ ($B_n^m$) is important in $R_2Fe_{14}B$, we treat them as adjustable parameters to explain the observed results. To understand the role of each term in the CEF Hamiltonian we consider a simple case in which the exchange energy of Fe-$R$ interaction is much larger than the CEF potential energy of an $R$ ion. Thus all the moments are collinear. We employ Eq. (4) for the CEF Hamiltonian within the ground $J$ multiplet. Since the quantization axis coincides with $\mathbf{m}_0$ (antiparallel to $\mathbf{H}_m$), the anisotropy energy of the $R$ ion is expressed by

$$E_{an}(\theta,\phi)=\langle J,M=\mp J \mid \mathcal{H}_R \mid J,M=\mp J\rangle-\text{const} , \quad (31)$$

where $M=-J$ or $=+J$ for light $R$ or heavy $R$, respectively. The expectation value of the $B_n^m O_n^m$ term is given by

$$B_n^m\langle J,M=\mp J \mid O_n^m \mid J,M=\mp J\rangle = B_n^m f_n(J)F_n^m(\theta)G_m(\phi) , \quad (32)$$

where

$$f_2(J)=J(J-\tfrac{1}{2}) , \quad (33a)$$

$$f_4(J)=J(J-\tfrac{1}{2})(J-1)(J-\tfrac{3}{2}) , \quad (33b)$$

$$f_6(J)=J(J-\tfrac{1}{2})(J-1)(J-\tfrac{3}{2})(J-2)(J-\tfrac{5}{2}) , \quad (33c)$$

$$F_2^0(\theta)=-3\sin^2\theta , \quad (34a)$$

$$F_2^{-2}(\theta)=\sin^2\theta , \quad (34b)$$

$$F_4^0(\theta)=35\sin^4\theta-40\sin^2\theta , \quad (34c)$$

$$F_4^{-2}(\theta)=-7\sin^4\theta+6\sin^2\theta , \quad (34d)$$

$$F_4^4(\theta)=\sin^4\theta , \quad (34e)$$

$$F_6^0(\theta)=-231\sin^6\theta+378\sin^4\theta-168\sin^2\theta , \quad (34f)$$

$$F_6^{-2}(\theta)=33\sin^6\theta-48\sin^4\theta+15\sin^2\theta , \quad (34g)$$

$$F_6^4(\theta)=-11\sin^6\theta+10\sin^4\theta , \quad (34h)$$

$$F_6^{-6}(\theta)=\sin^6\theta , \quad (34i)$$

$$G_0(\phi)=1 , \quad (34j)$$

$$G_2(\phi)=\sin 2\phi , \quad (34k)$$

$$G_4(\phi)=\cos 4\phi , \quad (34l)$$

$$G_6(\phi)=\sin 6\phi . \quad (34m)$$

The functions $F_n^m(\theta)$ are shown in Fig. 3.

Thus the anisotropy energy per $R$ ion is given by

$$E_{an}(\theta,\phi) = \langle J,M=\mp J \mid \sum_{i=1}^{4}\mathcal{H}_{CEF}(i) \mid J,M=\mp J\rangle/4-\text{const}$$
$$= K_1\sin^2\theta+K_2\sin^4\theta+K_3\sin^4\theta\cos 4\phi + K_4\sin^6\theta+K_5\sin^6\theta\cos 4\phi , \quad (35)$$

where

$$K_1=-3f_2B_2^0-40f_4B_4^0-168f_6B_6^0 , \quad (36a)$$

$$K_2=35f_4B_4^0+378f_6B_6^0 , \quad (36b)$$

$$K_3=f_4B_4^4+10f_6B_6^4 , \quad (36c)$$

$$K_4=-231f_6B_6^0 , \quad (36d)$$

$$K_5=-11f_6B_6^4 . \quad (36e)$$

The $B_n^{-2}O_n^{-2}$ ($n=2,4,6$) and $B_6^{-6}O_6^{-6}$ terms are canceled out owing to the relations $B_2^{-2}(1)=-B_2^{-2}(2)$, $B_2^{-2}(3)=-B_2^{-2}(4)$, etc.

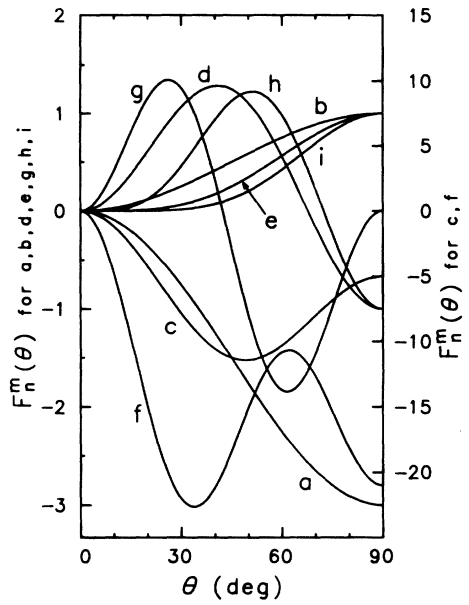


FIG. 3. The $\theta$ dependence of the expectation value of the Stevens operator $O_n^m$. $\langle O_n^m\rangle=f_n(J)F_n^m(\theta)G_m(\phi)$. *a*, $F_2^0(\theta)$; *b*, $F_2^{-2}(\theta)$; *c*, $F_4^0(\theta)$; *d*, $F_4^{-2}(\theta)$; *e*, $F_4^4(\theta)$; *f*, $F_6^0(\theta)$; *g*, $F_6^{-2}(\theta)$; *h*, $F_6^4(\theta)$; *i*, $F_6^{-6}(\theta)$.

The phenomenological expression identical with Eq. (35) is often used to interpret experimental results. It is, however, correct only in the limiting case of large $\mathbf{H}_m$ that the anisotropy constants $K_i$ can be expressed analytically in terms of the CEF coefficients $B_n^m$. In spite of the limited condition, an examination of the large $\mathbf{H}_m$ case is useful to understand the role of individual CEF term.

The easy direction of magnetization is determined usually by $K_1$ in Eq. (35). As seen from Eq. (36a) a negative $B_2^0$ is favorable for the easy $c$ axis and a positive one for the easy $c$ plane. Since the CEF strength $A_2^0$ arising from positive $R^{3+}$ charges are positive in $R_2Fe_{14}B$, signs of the Stevens factor $\alpha$ have explained the experimental results that magnetization vectors lie in the $c$ axis for the Pr, Nd (above $T_s$), Tb, Dy, and Ho (above $T_s$) compounds and in the $c$ plane for the Sm, Er, Tm, and Yb compounds below $T_s$.

Although $K_2$ and $K_3$ are expressed in terms of $B_4^0$ and $B_4^4$, respectively, in the approximation mentioned above, the situation is not so simple in $R_2Fe_{14}B$. When the magnitude of CEF energy is not very large relative to the Fe-$R$ exchange energy, the $B_2^{-2}$ term does not always vanish. As can be seen from Eqs. (32), (34b), and (34k), the magnetic moment of $R$ ion lies either in the [110] or in the [1$\bar{1}$0] direction, depending on the sign of $B_2^{-2}$. It is expected in the case of easy plane anisotropy that the four $R$ moments together with the 28 Fe moments form a noncollinear spin structure via the Fe-$R$ exchange interaction, as shown schematically in Fig. 4.[22] The resultant magnetization is parallel to the [100] direction. This noncollinear spin structure is expected for the Sm, Er, Tm, and Yb compounds. In fact, it has been confirmed for the Tm compound by neutron diffraction.[22] Thus the $B_2^{-2}O_2^{-2}$ term gives rise to the fourfold anisotropy energy

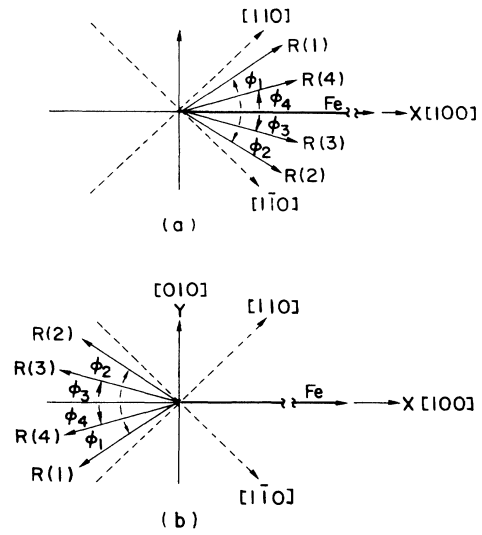


FIG. 4. Noncollinear spin structure in the (001) plane of $R_2Fe_{14}B$: (a) $R$=Sm, (b) $R$=Er,Tm,Yb.

in the $c$ plane, and is probably larger than that of the $B_4^4O_4^4$ term.

## IV. QUANTITATIVE RESULTS: SPIN STRUCTURE AND MAGNETIZATION PROCESS

On the basis of the qualitative consideration made in the preceding section, we have solved Eq. (6) numerically. The computation was made with the ACOS-1000 at Tohoku University. The main task is the diagonalization of matrices of $\mathcal{H}_R(i)$ given by Eqs. (7) and (13). For example, we consider a case in the Tm ($J$=6) compound to which an external field is applied along the [001] direction at low temperatures. To determine the equilibrium direction $\theta_0$ ($\phi_0$=0 in this case) of the Fe ion within an accuracy $\Delta\theta_0$=0.3°, we need to repeat the calculation of the free energy 30 to 40 times. For each time four $13\times13$ matrices of $\mathcal{H}_R(i)$ ($i$=1–4) must be diagonalized even when only the ground $J$ multiplet is taken into account.

Although there are many CEF parameters for an $R$ ion, the parameters of different $R$ ions can be related to each other, since $A_n^m(i)$ in Eq. (2) is nearly the same in all cases because of the almost identical lattice parameters. Of course, $B_n^m(i)$ and $C_n^m(i)$ are different for different $R$, as can be seen in Eqs. (5) and (19), respectively. In the previous work[24] we used a ratio defined by

$$b_n^m(i)=\frac{B_n^m(i)}{B_{n,p}^m(i)}=\frac{C_n^m(i)}{C_{n,p}^m(i)}=\frac{A_n^m(i)}{A_{n,p}^m(i)},\quad i=1,2,3,4\ , \tag{37}$$

where $B_{n,p}^m(i)$ [$C_{n,p}^m(i)$ and $A_{n,p}^m(i)$ also] is a calculated CEF coefficient arising from the point charges of the five nearest $R^{3+}$ ions only. The values of $A_{n,p}^m(i)$ for the Nd compound are given in Table II. The value of $A_{n,p}^m(R)$ for each $R$ compound is obtained by the relation $A_{n,p}^m(R)=A_{n,p}^m(\mathrm{Nd})(a_{\mathrm{Nd}}/a_R)^{n+1}$, where $a_R$ is the lattice constant of $R_2Fe_{14}B$. From the symmetry of the CEF it is obvious that $b_n^m(1)=b_n^m(2)=b_n^m(f)$ and $b_n^m(3)=b_n^m(4)=b_n^m(g)$. For simplicity we assumed $b_n^m(f)=b_n^m(g)\equiv b_n^m$. For the heavy $R$ compounds ($R$=Tb, Dy, Ho, Er, and Tm), the magnetization curves and the spin reorientation (SR) were explained almost satisfactorily within the ground $J$ multiplet in terms of the same set of parameters, that is, $H_m$=145 K, $b_2^0$=0.15, $b_2^{-2}$=0.2, and $b_4^m$=4 ($m$=0, −2,4).[24]

The possible set of parameters is not unique, but there are many other choices. The above magnetization curves can be reproduced by the same CEF parameters for $f$ and $g$ sites, that is, by assuming $A_n^m(f)=A_n^m(g)\equiv A_n^m$. In order to reconcile with the above assumption of $b_n^m(f)=b_n^m(g)\equiv b_n^m$, we have to assume $A_n^m\equiv b_n^m[A_{n,p}^m(f)+A_{n,p}^m(g)]/2$. However, in the present work, for simplicity, we assumed that $b_n^m$ is redefined by

$$b_n^m=\frac{A_n^m(i)}{A_{n,p}^m(i)},\quad i=1,2\ . \tag{38}$$

The CEF and molecular field parameters, $A_n^m(b_n^m)$ and $H_m$, used in the present work are given in Table III.

### A. $R_2Fe_{14}B$ with heavy $R$ elements

For the compounds of heavy $R$ ($R$=Tb, Dy, Ho, Er, and Tm), the magnetization curves and spin reorientation are explained almost satisfactorily within the ground $J$ multiplet in terms of the same set of parameters given in Table III, that is, $H_m$=145 K, $b_2^0$=0.15, $b_2^{-2}$=0.2, $b_4^0$=2, $b_6^0$=−20, and $b_6^{-6}$=−25. The calculated and observed magnetization curves are shown in Fig. 5, and the SR temperatures are listed in Table IV. For the Ho compound, the spin tilting angle of about 23° from the $c$ axis at 4.2 K (Ref. 5) is also well reproduced. Although there are no measurements on single crystals of the Yb compound, the result of calculation is also shown in Fig. 5 for reference. For all the heavy $R$ compounds except $R$=Ho, the observed results can also be reproduced satisfactorily in terms of only the two parameters $B_2^0$ and $B_2^{-2}$ as described previously for the Tm compound.[22] In that work we assumed that the temperature dependence of $K_0(T)$ is proportional to $[m_0(T)]^2$. The present work used the observed $K_0(T)$ of the Y compound which has a maximum at about 300 K.[5] This anomalous behavior of $K_0(T)$ has an influence on the calculated value of $T_s$.

TABLE II. Calculated CEF coefficients $A_{n,p}^m$ (in units of $Ka_0^{-n}$, $a_0$: Bohr radius) for $f_1$ and $g_1$ sites of $Nd_2Fe_{14}B$ arising from the point charges of the only five nearest $R^{3+}$ ions. The signs of $A_{n,p}^{-2}$ ($n$=2,4,6) and $A_{6,p}^{-6}$ for $f_2$ and $g_2$ sites are opposite to those for $f_1$ and $g_1$ sites, respectively.

| Site | $A_{2,p}^0$ | $A_{2,p}^{-2}$ | $A_{4,p}^0$ | $A_{4,p}^{-2}$ | $A_{4,p}^4$ | $A_{6,p}^0$ | $A_{6,p}^{-2}$ | $A_{6,p}^4$ | $A_{6,p}^{-6}$ |
|---|---|---|---|---|---|---|---|---|---|
| $f_1$ | 1970 | −2270 | −6.13 | 18.6 | −23.6 | 0.0460 | −0.245 | 0.199 | −0.838 |
| $g_1$ | 2640 | 795 | −9.54 | −7.67 | 16.1 | 0.0808 | 0.139 | −0.239 | −1.69 |

The spin reorientation in the Er, Tm, and Yb compounds occurs as either the first- or the second-order transition, depending on the values of parameters. Even in the case of the second-order transition, however, the temperature range over which the spins rotate is only within a few degrees. Hence we did not make a more detailed study of this problem.

As is seen in Fig. 5, the observed magnetizations of the Ho, Er, and Tm compounds in the hard direction increase monotonically with increasing field up to 145 kOe without any indication of saturation at 4.2 K. At room temperature, however, they saturate at about 100 kOe for

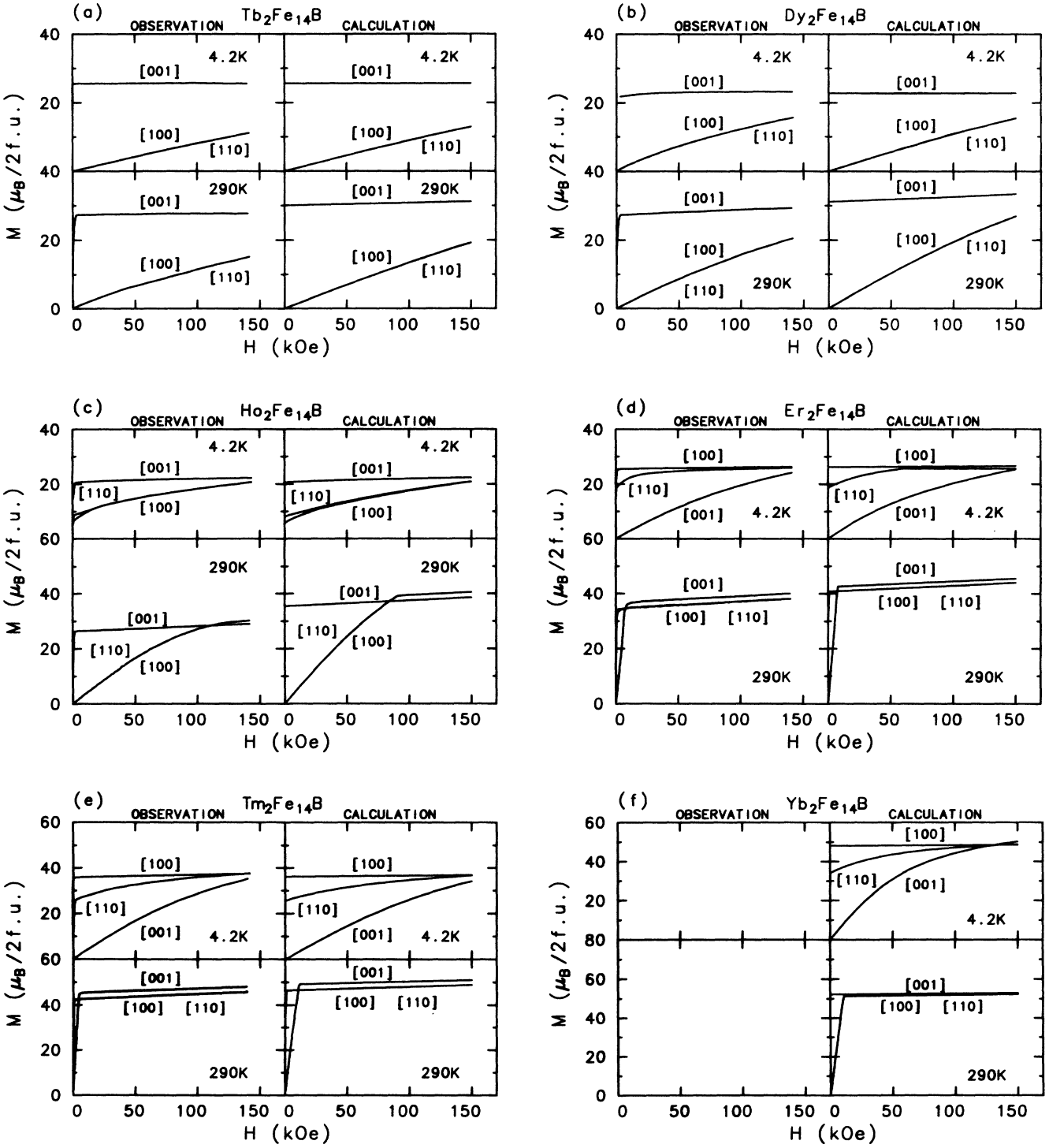


FIG. 5. Observed (Refs. 24 and 49) and calculated magnetization curves for the heavy $R$ compounds: (a) $R$=Tb, (b) $R$=Dy, (c) $R$=Ho, (d) $R$=Er, (e) $R$=Tm, (f) $R$=Yb. The calculation for different materials is based on the same parameters given in Table III: $b_2^0=0.15$, $b_2^{-2}=0.2$, $b_4^0=2$, $b_6^0=-20$, $b_6^4=-25$, $b_4^{-2}=b_4^4=b_6^{-2}=b_6^6=0$, and $H_m=145$ K.

TABLE III. CEF and molecular field parameters $A_n^m$ (in units of $Ka_0^{-n}$) and $H_m$ (K) of $R_2Fe_{14}B$ used in the present work. The value in parentheses is the ratio given by $b_n^m = A_n^m / A_{n,p}^m$, where $A_{n,p}^m$ is the CEF coefficient for $f_1$ site given in Table II.

| $R$ | $A_2^0$ ($b_2^0$) | $A_2^{-2}$ ($b_2^{-2}$) | $A_4^0$ ($b_4^0$) | $A_4^{-2}$ ($b_4^{-2}$) | $A_4^4$ ($b_4^4$) | $A_6^0$ ($b_6^0$) | $A_6^{-2}$ ($b_6^{-2}$) | $A_6^4$ ($b_6^4$) | $A_6^{-6}$ ($b_6^{-6}$) | $H_m$ |
|---|---|---|---|---|---|---|---|---|---|---|
| Pr | 295 | −454 | −12.3 | | | −6.89 | −14.7 | −29.8 | 25.1 | 300 |
| | (0.15) | (0.2) | (2.0) | | | (−150) | (60) | (−150) | (−30) | |
| Nd | 295 | −454 | −12.3 | | | −1.84 | 9.80 | −15.9 | | 350 |
| | (0.15) | (0.2) | (2.0) | | | (−40) | (−40) | (−80) | | |
| Sm | 297 | −458 | −12.4 | | | −7.95 | | −20.2 | | 230 |
| | (0.15) | (0.2) | (2.0) | | | (−170) | | (−100) | | |
| Tb | 300 | −462 | −12.6 | | | −0.958 | | −5.17 | | 145 |
| | (0.15) | (0.2) | (2.0) | | | (−20) | | (−25) | | |
| Dy | 302 | −467 | −12.7 | | | −0.973 | | −5.29 | | 145 |
| | (0.15) | (0.2) | (2.0) | | | (−20) | | (−25) | | |
| Ho | 302 | −467 | −12.7 | | | −0.973 | | −5.29 | | 145 |
| | (0.15) | (0.2) | (2.0) | | | (−20) | | (−25) | | |
| Er | 303 | −471 | −12.8 | | | −0.980 | | −5.33 | | 145 |
| | (0.15) | (0.2) | (2.0) | | | (−20) | | (−25) | | |
| Tm | 303 | −471 | −12.8 | | | −0.980 | | −5.33 | | 145 |
| | (0.15) | (0.2) | (2.0) | | | (−20) | | (−25) | | |
| Yb | 303 | −471 | −12.8 | | | −0.980 | | −5.33 | | 145 |
| | (0.15) | (0.2) | (2.0) | | | (−20) | | (−25) | | |

the Ho compound and at 5 kOe for the Er and Tm compound, although the saturation values are different from those of the easy directions. Our calculations elucidate, quite satisfactorily, the difference of the magnetization processes between 4.2 and 290 K.

Figure 6 shows the calculated magnetization curves of the three directions of the Tm compound in the magnetic fields up to 1800 kOe at $T=0$ K. The [001] magnetization increases monotonically with increasing field across the [100] and [110] curves above 150 kOe, and approaches the expected magnetization value of the ferromagnetic ordering of Fe and $R$ sublattices. The [100] and [110] curves show the FOMP accompanied with an abrupt transition from the ferrimagnetic to ferromagnetic ordering. The noncollinear spin structure still remains after the transition. This transition has not yet been found experimentally, although an incipient stage was observed.[8]

### B. $R_2Fe_{14}B$ with light $R$ elements

The situation for the light $R$ compounds is not so simple as the heavy $R$ compounds. For example, the first excited $^6H_{7/2}$ multiplet of a free $Sm^{3+}$ ion lies at a distance of only 1225 K above the ground $^6H_{5/2}$ multiplet. When the paramagnetic $Sm^{3+}$ ion is subjected to an external magnetic field, the Zeeman term causes mixing of the excited multiplet, which contributes significantly to the paramagnetic susceptibility even at low temperatures.[35] The effect of excited $J$ multiplets of $Sm^{3+}$ ion subjected simultaneously to a CEF and an exchange field has been discussed by several authors,[29–31,36,37] who lay emphasis on the mixing of multiplet via the CEF. In this study we note the importance of the mixing of multiplets caused by the exchange interaction $2\mathbf{S}\cdot\mathbf{H}_m$ especially in the Sm compounds and also in the Nd and Pr compounds. For a light $R^{3+}$ ion, the expectation value $\langle S_z \rangle = (1-g_J)J$ is smaller than $S$ within the ground $J$ multiplet. The mixing of the excited multiplet increases the expectation value $\langle S_z \rangle$, and lowers the expectation value of the exchange energy $2\mathbf{S}\cdot\mathbf{H}_m$.

TABLE IV. Calculated and observed spin reorientation temperature $T_s$ (K) of the heavy $R$ compounds.

| $R$ | Ho | Er | Tm | Yb |
|---|---|---|---|---|
| $T_s$(cal) | 56 | 328 | 343 | 210 |
| $T_s$(obs) | 58[a] | 323[a] | 315[a] | 115[b] |

[a]Reference 5.
[b]Reference 11.

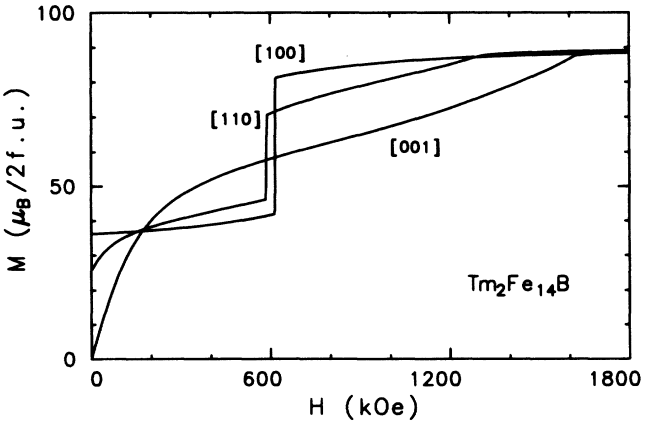


FIG. 6. Calculated magnetization curves for $Tm_2Fe_{14}B$ at 0 K in external fields up to 1800 kOe. The [100] and [110] curves show FOMP accompanied with transition from the ferrimagnetic to ferromagnetic ordering.

### 1. $Sm_2Fe_{14}B$

In the Sm compound the effect mentioned above causes remarkable influence on the spin structure and magnetization process. To illustrate the influence of the excited $J$ multiplet more specifically we consider a case in which the parameters given in Table III are assumed and the $J=\frac{5}{2}$ and $\frac{7}{2}$ multiplets with $\lambda=350$ K are taken into account. The ground-state wave function $|1\rangle$ of an $R(1)$ ion is given by

$$|1\rangle=\sum_{J=5/2,7/2}\sum_{M=-J}^{J}a_{JM}(1)|J,M\rangle\ ,$$
$$\sum_{J=5/2,7/2}\sum_{M=-J}^{J}|a_{JM}(1)|^2=1\ . \tag{39}$$

The magnetic moment (in units of $\mu_B$) of the $R(1)$ ion calculated by Eqs. (27)–(30) is

$$\begin{aligned}m_{1x}&=m_{1x}(J=\tfrac{5}{2})+m_{1x}(J=\tfrac{7}{2})-\delta S_{1x}\\&=0.646+0.118-0.474\\&=0.291\ ,\end{aligned} \tag{40}$$

$$\begin{aligned}m_{1y}&=m_{1y}(J=\tfrac{5}{2})+m_{1y}(J=\tfrac{7}{2})-\delta S_{1y}\\&=0.156+0.057+0.007\\&=0.220\ ,\end{aligned} \tag{41}$$

$$m_1=(m_{1x}^2+m_{1y}^2)^{1/2}=0.365\ . \tag{42}$$

When only the ground multiplet is taken into account, we obtain $m_{1x}=0.700$, $m_{1y}=0.129$, and $m_1=0.712$ which is close to the free ion value $g_JJ=0.714$.

In Eqs. (40) and (41), the first and second terms represent the magnetic moments belonging to the $J=\frac{5}{2}$ and $\frac{7}{2}$ multiplets, respectively. The third terms, $-\delta S_\gamma$ given by Eq. (29), represent the magnetic moment arising from the intermultiplet interaction. The results are shown in Fig. 7. The vector $-\delta\mathbf{S}$ is almost parallel to the molecular field $\mathbf{H}_m$, which means that this induced magnetic moment lowers the exchange energy considerably. The short dashed line with arrow in Fig. 7 represents the magnetic moment of the $R(1)$ ion in the case in which only the ground $J$ multiplet is taken into account. The $-\delta\mathbf{S}$ term markedly reduces[36,37] the magnetic moment of the Sm ion and considerably enhances the noncollinearity between the spins.

When an external field is applied along the [001] direction, the $-\delta\mathbf{S}$ term causes peculiar rotation of the magnetic moment of the Sm ion. The magnetic moment of the Sm ion rotates toward the $[00\bar{1}]$ direction at first, i.e., opposite to the direction of $\mathbf{H}$, and then it returns back when the field is further increased.

The influence of the excited multiplets on the spin structure of the Sm compound is more pronounced at higher temperatures. The calculated spin structures at $T=0$, 290, and 400 K are shown in Fig. 8 for the three cases where the multiplet(s) of (a) $J=\frac{5}{2}$, (b) $J=\frac{5}{2}$ and $\frac{7}{2}$, (c) $J=\frac{5}{2}$, $\frac{7}{2}$, and $\frac{9}{2}$ are taken into account. The parameters used in the calculation are given in Table III. The transition from ferromagnetism to ferrimagnetism in keeping the noncollinear spin structure will occur in the Sm compound with increasing temperature.

When an external field is applied along the [001] direction the magnetic moments of Fe ions rotate simply from [100] toward [001], while the magnetization process of Sm ions is complicated, depending on whether or not the excited $J$ multiplets are taken into account in the calculation. At $T=0$ K, the noncollinear ferromagnetic spin structure in the (001) plane shown in Fig. 8 changes to the collinear ferromagnetic structure in the [001] direction at the saturation field of about 1000 kOe. On the

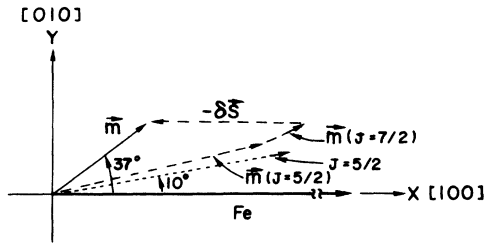


FIG. 7. Influence of the first excited $J$ multiplet on the magnetic moment of Sm ion of $Sm_2Fe_{14}B$: $\mathbf{m}(J=\frac{5}{2})$ and $\mathbf{m}(J=\frac{7}{2})$ represent the magnetic moments belonging to the $J=\frac{5}{2}$ and $\frac{7}{2}$ multiplets, respectively, $-\delta\mathbf{S}$ the magnetic moment arising from intermultiplet interaction, and $\mathbf{m}$ the resultant moment. The short dashed line with arrow represents the magnetic moment within the ground $J$ multiplet, which is very close to $g_JJ=0.714$. Parameters are given in Table III.

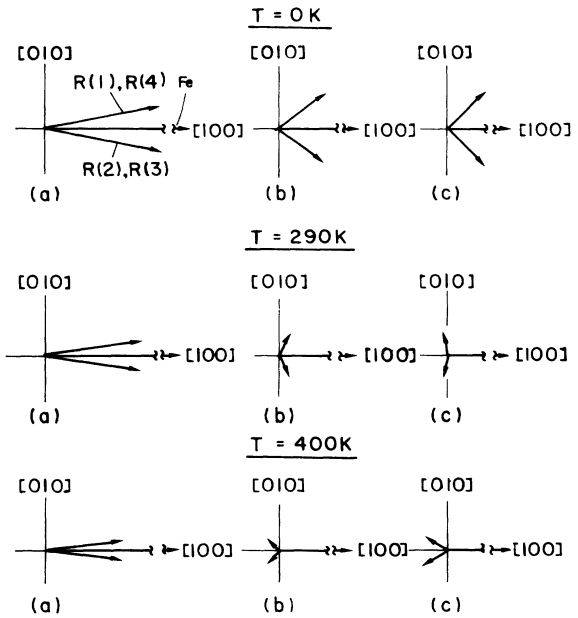


FIG. 8. Calculated spin structures of $Sm_2Fe_{14}B$ at $T=0$, 290, and 400 K for three cases where the multiplet(s) (a) $J=\frac{5}{2}$, (b) $J=\frac{5}{2}$ and $\frac{7}{2}$, (c) $J=\frac{5}{2}$, $\frac{7}{2}$, and $\frac{9}{2}$ are taken into account. We assumed the same CEF for both $f$ and $g$ sites, that is, $A_n^m(1)=A_n^m(4)$ and $A_n^m(2)=A_n^m(3)$, so that $\mathbf{m}_1=\mathbf{m}_4$ and $\mathbf{m}_2=\mathbf{m}_3$. The parameters are given in Table III.

other hand, at temperatures between 200 and 270 K, the noncollinear ferromagnetic spin structure in the (001) plane changes to the collinear ferrimagnetic structure in the [001] direction at the saturation field. In this case, the magnetic moments of the Sm ions rotate from the (001) plane toward the $[00\bar{1}]$ direction against the external field. At 400 K, the spin structure is already noncollinear ferrimagnetic in the (001) plane at $H=0$, and an external field in the [001] direction causes the collinear ferrimagnetic structure in the [001] direction.

The observed[12,38] and calculated magnetization curves of the Sm compound are shown in Fig. 9. The [001] curves are calculated for the three cases where the multiplet(s) of (a) $J=\frac{5}{2}$, (b) $J=\frac{5}{2}$ and $\frac{7}{2}$, (c) $J=\frac{5}{2}$, $\frac{7}{2}$, and $\frac{9}{2}$ are taken into account. The influence of the excited $J$ multiplets on the magnetization is evident. The anomalous increase in the [001] curve above 200 kOe arises from the sixth-order CEF terms whose effect appears only through the excited $J$ multiplets because the sixth-order Stevens factor $\gamma$ is zero for a $Sm^{3+}$ ion. The values of $b_2^{-2}$ larger than 0.2 give rise to a better agreement with the observed [110] curve without affecting the other curves.

### 2. $Nd_2Fe_{14}B$

The magnetization vector of the Nd compound tilts at about 32° from the [001] to the [110] direction at 4.2 K.[4] The tilting angle decreases monotonically with increasing temperature and becomes zero at about 135 K, much higher than that in the Ho compound (58 K).[5] The magnetization measured by Kajiwara *et al.*[16,17] showed a sudden jump in the [100] direction at about $H_j=170$ kOe, but no anomalous change was observed in the [110] direction up to 300 kOe. After the jump, the magnetization vector seems to lie in the [100] direction.

Our calculations show that the spin structure below $T_s$ is noncollinear but all magnetic moments of Fe and Nd ions lie in the $(1\bar{1}0)$ plane, i.e., $\phi_0=\phi_i=45°$ $(i=1-4)$, and $|\theta-\theta_i|$ is of the order of a degree. The SR temperature $T_s$ depends strongly on the strength of molecular field $H_m$ acting on the Nd ion. To reproduce the observed $T_s$ it is necessary to take much larger $H_m$ than that for the heavy $R$ compounds. A conventional phenomenological theory which assumes the anisotropy energy given by Eq. (35) requires the sixth-order anisotropy energy terms to produce a jump in the magnetization curve in this case. In our model the jump in the [100] curve can be reproduced in terms of the CEF coefficients up to fourth order. By inspecting Eqs. (34) and Fig. 3, we find out that the $A_4^{-2}$ term is favorable for such a jump. For example, a set of parameters $H_m=350$ K, $b_2^0=0.39$, $b_2^{-2}=0.85$, $b_4^0=7.8$, $b_4^{-2}=16$, and $b_4^4=15$, which reproduces the zero-field tilting angle $\theta_0=32°$ at 0 K, gives rise to a jump in the [100] direction at $H_j=135$ kOe. The SR temperature, however, is 65 K, much lower than the observed value, which is due to the shallow minimum of the free energy.

In order to make the free-energy minimum deeper at about $\theta_0=32°$ for $H=0$ and to stabilize it, $A_6^0(b_6^0)$ term is necessary, and $A_6^4(b_6^4)$ term is also favorable for the jump in the [100] direction as can be seen from Eqs. (34) and Fig. 3. The results of calculations are shown in Fig. 10, where the parameters given in Table III are used and the ground and first excited $J$ multiplets are taken into account. This set of parameters yields the values $\theta_0=31°$, $H_j=160$ kOe, and $T_s=130$ K, and a larger value of $A_2^0$ $(b_2^0=0.16-0.17)$ yields a field closer to the observed $H_j=170$ kOe. A similar set of parameters has been obtained by Li,[25] without taking account of the excited $J$ multiplets.

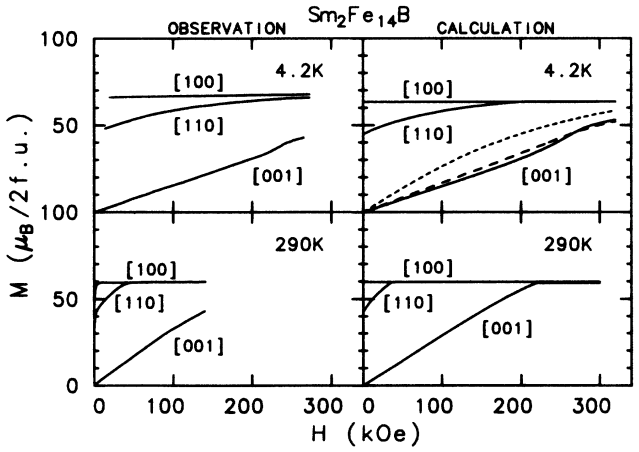


FIG. 9. Observed (Refs. 12 and 38) and calculated magnetization curves for $Sm_2Fe_{14}B$. The solid lines represent the results in which ground $(J=\frac{5}{2})$, first $(J=\frac{7}{2})$, and second $(J=\frac{9}{2})$ excited multiplets are taken into account. The long dashed and short dashed lines represent the [001] curves in which $J=\frac{5}{2}$ and $\frac{7}{2}$ multiplets and $J=\frac{5}{2}$ multiplet are taken into account, respectively. Parameters used in the calculation are given in Table III.

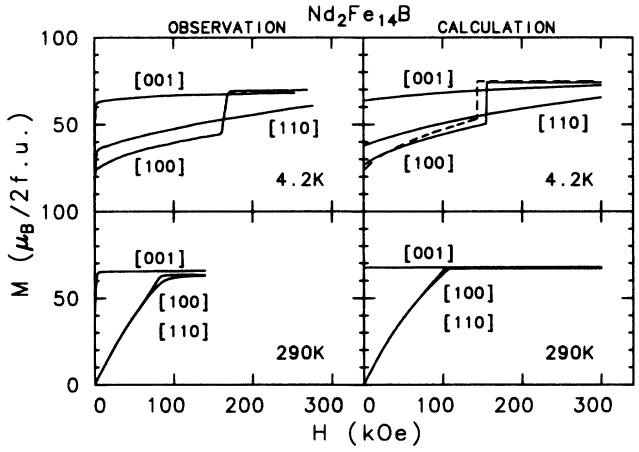


FIG. 10. Observed (Refs. 16 and 17) and calculated magnetization curves for $Nd_2Fe_{14}B$. Solid lines represent the results in which the ground $(J=\frac{9}{2})$ and first excited $(J=\frac{11}{2})$ multiplets are taken into account, while long dashed lines the results including the ground multiplet only. Parameters are given in Table III.

### 3. $Pr_2Fe_{14}B$

For the Pr compound whose magnetization curve at room temperature is similar to that of the Nd compound, the spin direction remains parallel to the $c$ axis even at 4.2 K. Recently Hiroyoshi *et al.*[18] observed the FOMP in both [100] and [110] directions at low temperatures. Magnetization jumps occur at about 130 and 160 kOe in the [100] and [110] directions, respectively. After the abrupt increase, however, the magnetization does not reach the easy direction value, in marked contrast to the case of the Nd compound. An inspection of Eqs. (34) and Fig. 3 suggests that $A_6^0$ term is favorable for such transitions. The magnetization curves calculated using the parameters in Table III are shown in Fig. 11. The solid lines represent the results in which the ground $J=4$ and the first excited $J=5$ multiplets are taken into account, while long dashed lines include only the ground multiplet. Calculated values of $H_j$ are 145 and 180 kOe in the [100] and [110] directions, respectively. A better agreement with the experiment is obtained with a value of $A_2^0(b_2^0)$ smaller than that given in Table III.[18] The influence of the excited multiplet on the magnetization curve is remarkable near the transition field; it enlarges the discontinuous change of the magnetization at $H_j$.

It is of significance to mention the difference in the magnetization process between the [100] and [110] directions. When the field is applied along the [100] direction, the magnetic moments of Fe ions rotate from [001] toward [100] within the (010) plane while the $R$ moments at $f_1(g_2)$ and $f_2(g_1)$ sites show different behavior because the easy direction of the $R$ ions in the $c$ plane is either [110] or [1$\bar{1}$0] direction, hence the noncoplanar magnetic structure is realized. If the direction of each moment is specified by polar angles $(\theta_0,\phi_0)$ for the Fe moment, and by $(\theta_1,\phi_1)$ and $(\theta_2,\phi_2)$ for the $R$ moments at $f_1$ and $f_2$ sites, respectively, the relations $\phi_0=0$, $-\phi_1=\phi_2$, and $\theta_0\neq\theta_1=\theta_2$ are fulfilled. When the field is applied along the [110] direction, on the other hand, all moments are coplanar in the (1$\bar{1}$0) plane, although they are still noncollinear, namely, $\phi_0=\phi_1=\phi_2=45°$ and $\theta_0\neq\theta_1\neq\theta_2$. The field dependence of the polar angles and the magnetic moments of $R$ ions are shown in Fig. 12, when the field is applied along the [100] direction.

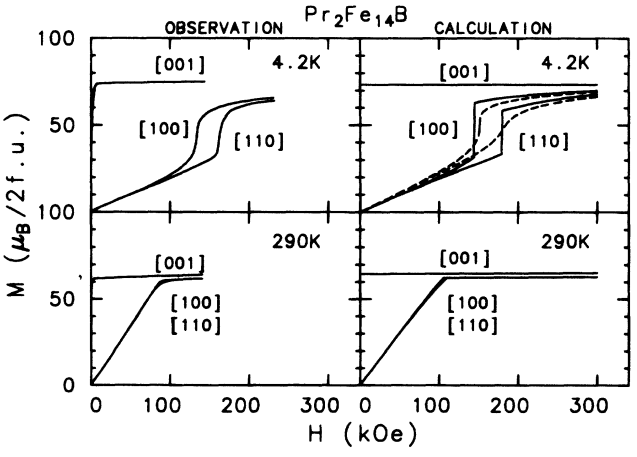


FIG. 11. Observed (Ref. 18) and calculated magnetization curves for $Pr_2Fe_{14}B$. Solid lines represent the results in which the ground ($J=4$) and first excited ($J=5$) multiplets are taken into account, while long dashed lines the results including the ground multiplet only. Parameters are given in Table III.

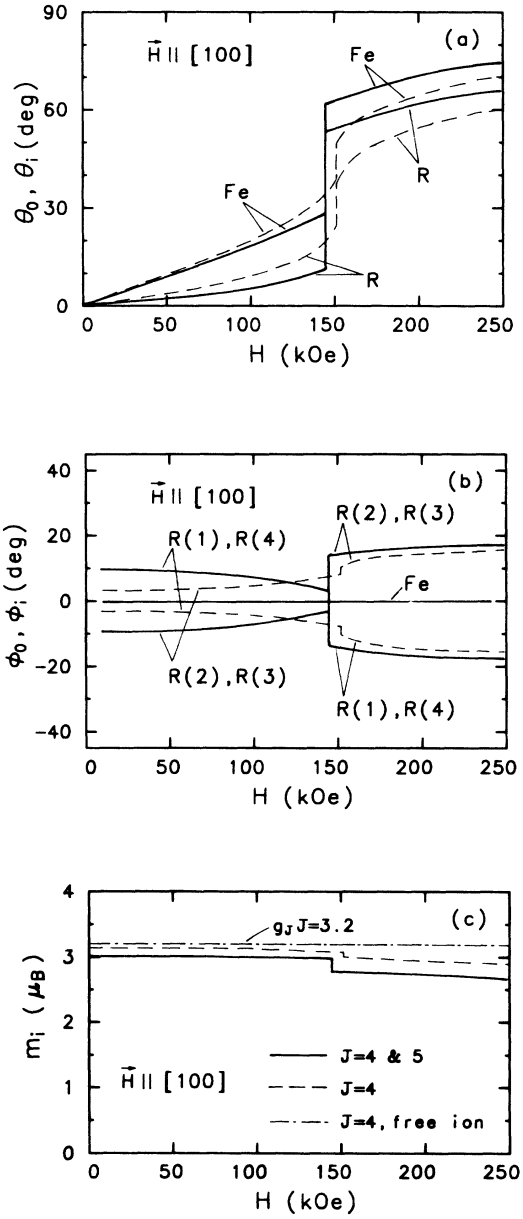


FIG. 12. Field dependence of the magnetic moments of $Pr_2Fe_{14}B$ at 0 K when an external field $H$ is applied along the [100] direction: Fe moment $\mathbf{m}_0=(m_0=2.2\mu_B,\theta_0,\phi_0=0)$, $R$(Pr) moment $\mathbf{m}_i=(m_i,\theta_i,\phi_i)$, $i=1$–4. The solid lines represent the results in which the ground ($J=4$) and first excited ($J=5$) multiplets are taken into account, while long dashed line the results including the ground multiplet only. (a) $\theta_0,\theta_i$ vs $H$, (b) $\phi_0,\phi_i$ vs $H$, (c) $m_i$ vs $H$ ($m_i$ is independent of $i$). The chain line represents the free-ion value for the ground multiplet.

## V. DISCUSSION

The magnetic anisotropy in $R_2Fe_{14}B$ is understood satisfactorily through the study of $R$ ion subjected to a crystalline electric field combined with an exchange field. This success comes from the fortunate circumstances in $R_2Fe_{14}B$ where the contribution of $R$ ions can be separated from that of Fe ions. We can obtain the information about the Fe sublattice from the observed results of the Y compound. It should be recognized that the rare-earth metals are transition elements and they will contribute something to the magnitude of Fe moment and the interaction between Fe moments. This contribution, however, has been ignored in the present paper except that the temperature dependence of $H_m$ is corrected so as to reproduce the observed Curie temperature for each $R_2Fe_{14}B$.

In the Ce compound, like the Y compound, it appears that the Ce ion is in the $Ce^{4+}$ state and only the Fe ions have the magnetic moments. The Curie temperature of the Ce compound, $T_c=422$ K, much lower than that of other $R$ compounds seems to arise from the influence of the $Ce^{4+}$ state on the Fe sublattice.

Although we have assumed the same CEF potential for both $f$ and $g$ sites, different potentials are indispensable for the two sites to explain the spin structure observed by neutron diffraction.[22] But as far as the magnetization is concerned, the distinction between $f$ and $g$ sites is not essential.

Present analysis has shown that a systematic description of the magnetization process in $R_2Fe_{14}B$ is possible when the CEF parameters are scaled to the point charge values, although larger sixth-order CEF parameters $b_6^m(A_6^m)$ are necessary for the light $R$ compounds rather than for the heavy $R$ compounds. Furthermore, for the light $R$ compounds, much larger molecular field $H_m$ is necessary to explain the observed results, especially for the high SR temperature of the Nd compound. Now we have no explanation for this large $H_m$ for the light $R$ compounds, although Cadogan *et al.*[39] have obtained similar results for $H_m$ by comparing experimental $T_c$ values. Moreover, the temperature dependence of the magnetization observed in the low-temperature range can be favorably explained by steeper decreasing of $H_m(T)$ rather than $m_0(T)$. These facts may be partly due to the $R$-$R$ exchange interaction which is neglected here.

The negative sign of $b_6^m$ for the Nd and Pr compounds means that the sign of the corresponding CEF potential is opposite to that arising from the point charges of neighboring $R^{3+}$ ions. Results of calculations,[20,40] which take also the point charges of Fe and B ions into account, do not consistently account for the required sign of $A_n^m$. Various interactions coming from a quantum-mechanical origin should contribute to CEF.[41–43] Molecular or covalent binding (and correlation or valence fluctuation might as well) tends to concentrate electric charge along bond lines connecting between nuclear centers. A modified (or extended) point-charge model[44] may possibly give rise to CEF parameters consistent with our prediction of $A_n^m$. It is worthwhile to point out that the values of $A_n^m$ ($n\leq 4$) are of the same order for all the $R$ compounds.

The FOMP observed for the Nd and Pr compounds show no hysteresis of the magnetization. Our calculation gives a maximum of the free energy between the two minima which have the same value at the transition field. The height of the potential barrier is about 5 K per two formula units for the Pr compound at $T=0$ K, so that the FOMP should exhibit a hysteresis if only the simultaneous rotation of the magnetization is permitted. There must exist some nucleation-growth mechanism to change the direction of the magnetization vector without loss of energy.

Next, the influence of the excited $J$ multiplets on the magnetization process should be discussed. The first excited $J$ multiplets of free $Nd^{3+}$ and $Pr^{3+}$ ions lie at 2300 and 2600 K, respectively, above the ground $J$ multiplet, which are considerably higher than 1225 K of $Sm^{3+}$. Hence, the influence of the excited multiplets on the spin structure and magnetization process will be very small in the Nd and Pr compounds as compared with the Sm compound. We assumed that in $R_2Fe_{14}B$ compounds the exchange energy $2\mathbf{S}\cdot\mathbf{H}_m$ for the $R$ ion is about $140\sim 350$ K, which is considerably larger than the Zeeman energy $(\mathbf{L}+2\mathbf{S})\cdot\mathbf{H}$. The nondiagonal matrix elements of $2\mathbf{S}\cdot\mathbf{H}_m$ between the ground and the first excited multiplets cause most of the mixing of the excited multiplet and the change of the free energy. When an external field is applied in the hard direction, the angle between $\mathbf{S}$ and $\mathbf{m}_0$ may increase, so that the scalar product $2\mathbf{S}\cdot\mathbf{H}_m$ may decrease with increasing field. This gives rise to a change in the matrix elements of $2\mathbf{S}\cdot\mathbf{H}_m$ between the ground and first excited multiplets. Thus the influence of the excited multiplet appears in the magnetization curve.

As seen in Fig. 11, this effect is very large in the vicinity of FOMP, where the free-energy curve of the system has two shallow minima when plotted against the direction of the magnetization vector. In this case the curvature around the minima is so small that a slight energy change arising from the matrix elements of $2\mathbf{S}\cdot\mathbf{H}_m$ between the ground and the excited multiplets causes rather a large change in positions of the minima, namely, the directions of the magnetization vector. When the magnitude of the field is far apart from that of FOMP, the free-energy curve has only one deep minimum. Thus only a slight change in the minimum position or the magnetization due to the excited multiplet is expected.

The above effect is much smaller for the heavy $R$ compounds because the first excited multiplet of heavy $R$ ion lies at higher energy level than that of the light $R$ ion, and moreover the expectation value $\langle S_z\rangle=(g_J-1)J$ is equal to $S$ for the heavy $R^{3+}$ ion, so that the $-\delta\mathbf{S}$ term, given by Eq. (29), arising from the mixing of excited states is expected to be negligibly small.

Finally in connection with the influence of mixing of the excited $J$ multiplets, we mention the concept of the anisotropic exchange interaction,[45–47] which is commonly used in the spectroscopic study of the rare-earth iron garnet (RIG).[45,48] The situation in RIG is similar to that in $R_2Fe_{14}B$: the Fe-Fe exchange interaction is much stronger than that of the Fe-$R$, and weaker $R$-$R$ interaction may be neglected. Much spectroscopic work has

been done on RIG. Optical absorption spectra of the $R$ ion determine the energy splitting of $R$ ion in the presence of CEF, external field, and exchange field. In traditional analyses, the splitting of Kramers doublet of $R$ ion is described in terms of $g$ tensor and exchange field tensor in the framework of the effective spin $S=\frac{1}{2}$.[46–50] The anisotropic exchange means that the two tensors do not have the same anisotropy.[48] To explain the observed optical absorption spectra, the anisotropy of exchange field is indispensable, if we approach the problem in this manner. In our treatment of the $R$ ion in $R_2Fe_{14}B$, on the other hand, $\sum(2J+1)\times\sum(2J+1)$ matrices of the Hamiltonian Eq. (13) are diagonalized to obtain the energy splitting. Then the anisotropy of the molecular field due to $\lambda\mathbf{L}\cdot\mathbf{S}$ is taken into account automatically.

Thus we can explain the magnetic behavior of $R_2Fe_{14}B$ quite successfully. The same treatment is applicable to $R_2Co_{14}B$. Recently Hiroyoshi *et al.*[14] have observed FOMP in $Nd_2Co_{14}B$. Detailed analysis of the magnetic properties of $R_2Co_{14}B$ will be published elsewhere.

## ACKNOWLEDGMENTS

The authors are much indebted to Dr. H. Hiroyoshi, Dr. H. Yamauchi, Dr. G. Kido, and Dr. Y. Yamaguchi of Tohoku University, and also to Dr. S. Hirosawa and Dr. M. Sagawa of Sumitomo Special Metals Co. Ltd. for their cooperation in this work.

[1]M. Sagawa, S. Fujimura, M. Togawa, H. Yamamoto, and Y. Matsuura, J. Appl. Phys. **55**, 2083 (1984).
[2]J. F. Herbst, J. J. Croat, F. E. Pinkerton, and W. B. Yelon, Phys. Rev. B **29**, 4176 (1984).
[3]D. Givord, H. S. Li, and J. M. Moreau, Solid State Commun. **50**, 497 (1984).
[4]D. Givord, H. S. Li, and R. Perrier de la Bathie, Solid State Commun. **51**, 857 (1984).
[5]S. Hirosawa, Y. Matsuura, H. Yamamoto, S. Fujimura, M. Sagawa, and H. Yamauchi, J. Appl. Phys. **59**, 873 (1986).
[6]N. C. Koon, B. N. Das, M. Rubinstein, and J. Tyson, J. Appl. Phys. **57**, 4091 (1985).
[7]M. Sagawa, S. Fujimura, H. Yamamoto, Y. Matsuura, and S. Hirosawa, J. Appl. Phys. **57**, 4094 (1985).
[8]H. Hiroyoshi, N. Saito, G. Kido, Y. Nakagawa, S. Hirosawa, and M. Sagawa, J. Magn. Magn. Mater. **54-57**, 583 (1986).
[9]M. Bogé, J. M. D. Coey, G. Czjzek, D. Givord, C. Jeandey, H. S. Li, and J. L. Oddou, Solid State Commun. **55**, 295 (1985).
[10]W. B. Yelon and J. F. Herbst, J. Appl. Phys. **59**, 93 (1986).
[11]P. Burlet, J. M. D. Coey, J. P. Gavigan, D. Givord, and C. Meyer, Solid State Commun. **60**, 723 (1986).
[12]H. Hiroyoshi, H. Yamauchi, Y. Yamaguchi, H. Yamamoto, Y. Nakagawa, and M. Sagawa, Solid State Commun. **54**, 41 (1985).
[13]H. Yamauchi, M. Yamada, Y. Yamaguchi, H. Yamamoto, S. Hirosawa, and M. Sagawa, J. Magn. Magn. Mater. **54-57**, 575 (1986).
[14]H. Hiroyoshi, M. Yamada, N. Saito, H. Kato, Y. Nakagawa, S. Hirosawa, and M. Sagawa, J. Magn. Magn. Mater. **70**, 337 (1987).
[15]L. Pareti, F. Bolzoni, and O. Moze, Phys. Rev. B **32**, 7604 (1985).
[16]S. Kajiwawa, G. Kido, Y. Nakagawa, S. Hirosawa, and M. Sagawa, J. Phys. Soc. Jpn. **56**, 829 (1987).
[17]G. Kido, S. Kajiwara, Y. Nakagawa, S. Hirosawa, and M. Sagawa, IEEE Trans. Magn. **MAG-23**, 3107 (1987); (unpublished).
[18]H. Hiroyoshi, H. Kato, M. Yamada, N. Saito, Y. Nakagawa, S. Hirosawa, and M. Sagawa, Solid State Commun. **62**, 475 (1987).
[19]K. W. H. Stevens, Proc. Phys. Soc. London, Sect. A **65**, 209 (1952).
[20]J. M. Cadogan and J. M. D. Coey, Phys. Rev. B **30**, 7326 (1984).
[21]E. B. Boltich and W. E. Wallace, Solid State Commun. **55**, 529 (1985).
[22]M. Yamada, Y. Yamaguchi, H. Kato, H. Yamamoto, Y. Nakagawa, S. Hirosawa, and M. Sagawa, Solid State Commun. **56**, 663 (1985).
[23]S. G. Sankar and K. S. V. L. Narasimhar, J. Magn. Magn. Mater. **54-57**, 530 (1986).
[24]M. Yamada, H. Kato, H. Hiroyoshi, H. Yamamoto, and Y. Nakagawa, J. Magn. Magn. Mater. **70**, 328 (1987).
[25]H. S. Li, Ph.D. thesis, University of Grenoble, 1987.
[26]A. J. Freeman and R. E. Watson, Phys. Rev. **127**, 2058 (1962).
[27]F. G. Wakim, M. Synek, P. Grossgut, and A. DaMommio, Phys. Rev. A **5**, 1121 (1972).
[28]R. Orbach, Proc. R. Soc. London, Ser. A **264**, 458 (1961).
[29]M. J. Weber and R. W. Bierig, Phys Rev. **134**, A1492 (1964).
[30]H. W. de Wijn, A. M. van Diepen, and K. H. J. Buschow, Phys. Rev. B **7**, 524 (1973).
[31]S. G. Sankar, V. U. S. Rao, E. Segal, W. E. Wallace, W. G. D. Frederick, and H. J. Garrett, Phys. Rev. B **11**, 435 (1975).
[32]G. Racah, Phys. Rev. **62**, 438 (1942); **63**, 367 (1943).
[33]D. J. Newman, Adv. Phys. **20**, 197 (1971).
[34]A. R. Edmonds, *Angular Momentum in Quantum Mechanics* (Princeton University Press, Princeton, N.J., 1960).
[35]J. A. White and J. H. van Vleck, Phys. Rev. Lett. **6**, 412 (1961).
[36]K. H. J. Buschow, A. M. van Diepen, and H. W. de Wijn, Phys. Rev. B **8**, 5134 (1973).
[37]H. W. de Wijn, A. M. van Diepen, and K. H. J. Buschow, Phys. Status Solidi B **76**, 11 (1976).
[38]G. Kido, H. Kato, M. Yamada, Y. Nakagawa, S. Hirosawa, and M. Sagawa, J. Phys. Soc. Jpn. **56**, 4635 (1987).
[39]J. M. Cadogan, J. M. D. Coey, J. P. Gavigan, D. Givord, and H. S. Li, J. Appl. Phys. **61**, 3974 (1987).
[40]S. Adam, Gh. Adam, and E. Burzo, J. Magn. Magn. Mater. **61**, 260 (1986).
[41]D. J. Newman, Adv. Phys. **20**, 197 (1971).
[42]B. R. Judd, Phys. Rev. Lett. **39**, 242 (1977).
[43]D. J. Newman, J. Phys. F **13**, 1511 (1983).
[44]Z. Zolnierek, J. Phys. Chem. Solids **45**, 523 (1984).
[45]K. A. Wickersheim and R. L. White, Phys. Rev. Lett. **8**, 483 (1962).
[46]P. M. Levy, Phys. Rev. **135**, A155 (1964).
[47]P. M. Levy, Phys. Rev. **177**, 509 (1969).
[48]E. Orlich and S. Hufner, Z. Phys. **232**, 418 (1970).
[49]R. F. Pearson, Proc. Phys. Soc. London **86**, 1055 (1965).
[50]R. M. White and R. L. White, Phys. Rev. Lett. **20**, 62 (1968).